analytical chemistry

pubs.acs.org/ac Article

Electrochemical Immunoassay for the Detection of SARS-CoV-2 Nucleocapsid Protein in Nasopharyngeal Samples

Isabelle C. Samper, Catherine J. McMahon, Melissa S. Schenkel, Kaylee M. Clark, Wisarut Khamcharoen, Loran B. R. Anderson, James S. Terry, Emily N. Gallichotte, Gregory D. Ebel, Brian J. Geiss, David S. Dandy, and Charles S. Henry*

Cite This: *Anal. Chem.* 2022, 94, 4712–4719 Read Online

ACCESS | Metrics & More | Article Recommendations | Supporting Information

ABSTRACT: Point-of-care (POC) methods currently available for detecting SARS-CoV-2 infections still lack accuracy. Here, we report the development of a highly sensitive electrochemical immunoassay capable of quantitatively detecting the presence of the SARS-CoV-2 virus in patient nasopharyngeal samples using stencil-printed carbon electrodes (SPCEs) functionalized with capture antibodies targeting the SARS-CoV-2 nucleocapsid protein (N protein). Samples are added to the electrode surface, followed by horseradish peroxidase (HRP)-conjugated detection antibodies also targeting the SARS-CoV-2 N protein. The concentration of the virus in samples is quantified using chronoamperometry in the presence of 3,3′5,5′-tetramethylbenzidine. Limits of detection equivalent to less than 50 plaque forming units/mL (PFU/mL) were determined with virus sample volumes of 20 μL. No cross-reactivity was detected with the influenza virus and other coronavirus N proteins. Patient nasopharyngeal samples were tested as part of a proof-of-concept clinical study where samples were also tested using the gold-standard real-time quantitative polymerase chain reaction (RT-qPCR) method. Preliminary results from a data set of 22 samples demonstrated a clinical specificity of 100% (n = 9 negative samples according to RT-qPCR) and a clinical sensitivity of 70% for samples with RT-PCR cycle threshold (Ct) values under 30 (n = 10) and 100% for samples with Ct values under 25 (n = 5), which complies with the World Health Organization (WHO) criteria for POC COVID-19 diagnostic tests. Our functionalized SPCEs were also validated against standard plaque assays, and very good agreement was found between both methods (R^2 = 0.9993, n = 6), suggesting that our assay could be used to assess patient infectivity. The assay currently takes 70 min from sampling to results.

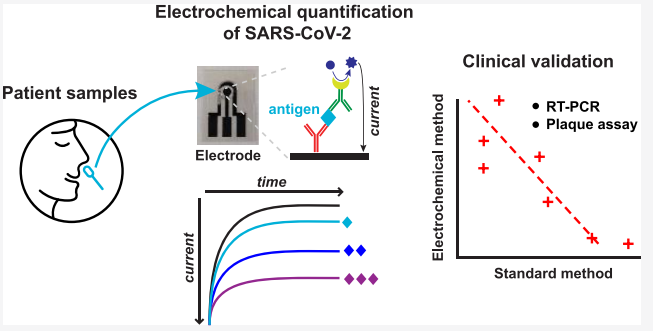

INTRODUCTION

Electrochemical sensors have received attention in recent years as a means of detecting biological analytes such as viruses and other disease-related pathogens, including HIV, the zika virus, and hepatitis B.[1−5] Detection mechanisms for the aforementioned pathogens have been integrated into point-of-care (POC) sensors, which can be deployable in low-resource settings, where standard instrumentation is not available. However, POC sensors can lack sensitivity and are usually only qualitative, as many of them use optical detection.[6,7] The incorporation of an electrochemical detection mechanism can improve sensitivity and provide quantitative measurements.

POC electrochemical biosensors have several advantages, including rapid response times, low limits of detection, and low sample volume requirements, while being cost-effective.[8] The most common examples are handheld glucometers, used by diabetic patients for routinely measuring their blood glucose levels.[9] In order to make electrochemical platforms suitable for POC applications, stencil-printed or screen-printed carbon electrodes (SPCEs) are often used, as they are robust, mass producible, and disposable.[10−12]

Coronavirus disease 2019, known as COVID-19, is caused by severe acute respiratory syndrome coronavirus 2 (SARS-CoV-2) and has impacted world health since late 2019. As of September 2021, the virus has infected 222 M people and resulted in 4.5 M deaths worldwide.[13] Prompt and accurate testing for SARS-CoV-2 and its mutations is essential for resuming social activities and ending the pandemic. Currently, the gold-standard viral test is real-time quantitative polymerase chain reaction (RT-qPCR), which is a molecular approach that amplifies the genetic material of the virus.[14,15] However, RT-qPCR can take several days to output results, and therefore,

Received: November 15, 2021
Accepted: March 1, 2022
Published: March 9, 2022

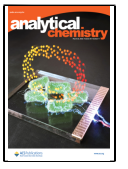

https://doi.org/10.1021/acs.analchem.1c04966
Anal. Chem. 2022, 94, 4712−4719

efforts have been made to build POC testing technologies to monitor the progression of the COVID-19 pandemic.[16,17] SARS-CoV-2 infection can also be detected with immunoassays, using antibodies to bind viral antigens with high specificity.[18] Enzyme-linked immunosorbent assays (ELISAs) are considered the standard for antigen testing; however, they are lab-based due to the need for external instrumentation to interpret the results.[19−21]

Monitoring of antibody and antigen levels plays a key role in assessing patient prognosis and managing the pandemic progression.[22,23] According to the Center of Disease Control (CDC), viral tests, including antigen tests, are valuable POC diagnostic tools to detect active infection and inform medical care.[24] Since the start of the pandemic, several antigen-based POC tests have been developed, with varying degrees of sensitivity, specificity, and accuracy. Two well-known and commercially available examples include the BinaxNOW test developed by Abbot and the InteliSwab test developed by OvaSure.[25,26] Several other POC tests have been developed, but their low sensitivities resulted in high rates of false negatives.[27]

To improve upon the current state of POC diagnostics for COVID-19, the sensitivity and accuracy of the test are of utmost importance. The incorporation of an electrochemical detection mechanism can provide an avenue to create a more robust, sensitive, and accurate POC diagnostic.[28,29] However, the development of POC technologies is not linear and requires several stages of development, including but not limited to the miniaturization of the sensing mechanism and the integration of reagent delivery, while also considering the means of sample collection, preparation, and addition to the diagnostic test to provide ease of use for the end user.[17] The work described herein focuses on the fundamental development of the sensing mechanism, including the ability to miniaturize the platform without compromising the immunoassay integrity. The goal of the proposed assay is to perform as well as standard ELISA but doing so outside of typical lab settings and without the long wait times and reagent high volumes.

Here, we present a novel electrochemical sandwich immunoassay using SPCEs to quantify the SARS-CoV-2 nucleocapsid protein (N protein) in nasopharyngeal samples. The N protein was chosen for this assay because of its clinical relevance in COVID-19 diagnostics.[30,31] SPCEs are functionalized with capture antibodies, which specifically bind to N proteins present in the sample tested. Detection antibodies conjugated to horseradish peroxidase (HRP) and the substrate, 3,3′5,5′-tetramethylbenzidine (TMB) are then added after the sample. Chronoamperometry is performed to measure the levels of HRP, which correlates to the N-protein concentration in the sample. Optimization of the immunoassay antibody pair is shown, and the sensor response to samples of varying virus concentrations is characterized. Additionally, cross-reactivity to variants and potential interferents is studied. Furthermore, a preliminary clinical study using 22 patient nasopharyngeal swab samples is conducted. Unlike other POC diagnostics, the method described here is quantitative, due to the use of an electrochemical measurement. This work is aimed at being the first step in developing a POC sensor for the rapid, sensitive, and accurate detection of active SARS-CoV-2 infection.

EXPERIMENTAL SECTION

Reagents. *Buffers.* 10 mM phosphate buffer solution (PBS) with 140 mM sodium chloride and 2.7 mM potassium chloride, pH 7.4 was prepared using a tablet according to package instructions (Research Products International, USA). 10 mM phosphate buffer solution with Tween20 (PBST) was made by adding Tween20 to PBS to a final concentration of 0.05%. Hanks Balanced Salt Solution (HBSS) was prepared by combining 0.14 M sodium chloride, 5 mM potassium chloride, 1 mM calcium chloride, 0.4 mM magnesium sulfate, 0.5 mM magnesium chloride, 0.3 mM sodium phosphate, 0.4 mM potassium phosphate, and 4 mM sodium carbonate to make a 1 L solution in Millipore water. HBSST buffer was made by adding Tween80 (Fischer Scientific, USA) and Igepal (MP Biomedicals, USA) to HBSS to make a final concentration of 0.1 and 0.1%, respectively. Viral transport media (VTM) were prepared according to CDC guidelines by adding fetal bovine serum, gentamicin sulfate, and amphotericin B to HBSS to a final concentration of 2%, 50, and 250 μg/mL, respectively.[32] VTMT was made by adding Tween80 and Igepal to VTM so that the final concentration of each surfactant was equal to 0.1%.

House-Made Anti-N Antibodies. Rabbit polyclonal antibodies targeting the SARS-CoV-2 N protein were prepared as previously described.[33,34] Briefly, rabbits were immunized by Pacific Immunology with the truncated SARS-CoV-2 nucleocapsid antigen (AA133-416) produced and purified in *Escherichia coli*. Hyperimmune serum was passed over a SARS-CoV-2 nucleocapsid column and binding antibodies eluted and collected. Eluted antibody preparations were dialyzed against PBS with 0.1% sodium azide and stored at −20 °C until use.

House-Made Anti-N-HRP. Anti-N antibodies prepared as described above were first purified using a NucAway spin column (Invitrogen by Thermo Fisher Scientific, USA) according to package instructions. Once purified, antibodies were conjugated to HRP using a Lightning-Link HRP Conjugation Kit (Abcam, UK) according to kit instructions. The stock antibody was diluted to 0.5 μg/mL in HBSST.

Aged Casein Solution. Solution was prepared as previously reported.[35] Briefly, a 100 mL solution was prepared by dissolving 6 g of casein in 80 mL of 50 mM sodium hydroxide overnight. Then, 0.26 g boric acid and 0.45 g sodium tetraborate were added, and the solution was pH adjusted to 8.5. The solution was brought to volume with Millipore distilled water and heated at 37 °C for 7 days. Aliquots of 50 μL were stored at −20 °C until needed and then thawed and combined with 950 μL of 50 mM borate buffer, pH 8.5 and mixed well.

Commercial Antibodies and Substrate. SARS-CoV-2 anti-N antibodies and SARS-CoV-2 anti-N-HRP detection antibodies (Table S1) were purchased from Sino Biological. Anti-N antibodies were diluted from the stock to 10 μg/mL in PBS, and HRP detection antibodies were diluted from the stock to 0.5 μg/mL in HBSST. The substrate TMB was purchased from Sigma-Aldrich, USA.

Inactivated SARS-CoV-2 Virus Samples. The SARS-CoV-2 virus (USA-WA1, NR52281) was provided by BEI resources. The virus was passaged at the biosafety level 3 (BSL-3) containment in Vero E6 cells [ATCC (CRL-1586)] in 2% FBS-DMEM at 37 °C to generate virus stocks. Virus stocks were stored at −80 °C. Viral stocks were quantified for

https://doi.org/10.1021/acs.analchem.1c04966
Anal. Chem. 2022, 94, 4712−4719

infectivity by the plaque assay [plaque forming units (PFU)/mL] and total genome copy number by real-time digital droplet polymerase chain reaction (RT-ddPCR), using the procedures established by Case et al.[36] To inactivate the virus, viral stocks were brought to a 0.1% final concentration of Triton-X-100 on ice for 30 min. All inactivated stocks were tested for the active virus using cytopathic effect assays of 5 days and were considered inactive if no cell killing was observed compared to live virus controls. All inactivated virus samples were handled following BSL2 safety practices. For the antibody screening study (Figure 1), virus samples were diluted in HBSST. For all other experiments, dilutions of the virus stock solution to the desired viral concentrations were made in VTMT.

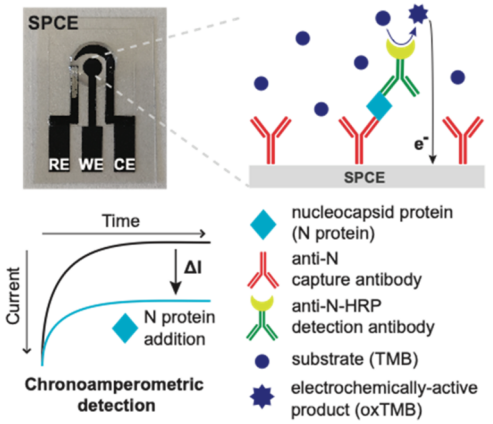

Figure 1. Electrochemical detection mechanism of the SARS-CoV-2 nucleocapsid (N) protein on a modified SPCE, with RE, WE, and CE representing reference, working, and counter electrodes, respectively. If present in the sample, N proteins are captured by anti-N antibodies (capture antibodies) immobilized on the SPCE surface. HRP-labeled anti-N antibodies (detection antibodies) subsequently bind to N proteins and catalyze the oxidation of the substrate TMB, creating an electroactive compound (oxTMB) that is detected via chronoamperometry.

Clinical Samples. Nasopharyngeal swabs were collected from asymptomatic staff at long-term care facilities and characterized as described here.[37] Briefly, viral RNA was extracted and quantified using qPCR with CDC primer probes. The infectious virus was measured using a standard plaque assay on Vero cells starting with 250 μL of input material. Clinical samples were surfactant-inactivated, which breaks up viral particles and releases N proteins in solution. Samples were diluted by a 1.07 factor in VTM, Tween80, and Igepal so that the final concentrations of Tween80 and Igepal in each sample were both equal to 0.1%. A 20 μL volume of each surfactant-containing clinical sample was tested on our immunoassay.

Electrode Fabrication. Electrodes were fabricated as previously reported.[38] Briefly, TC303 synthetic graphite (Asbury Carbons, USA) and carbon ink (Ercon, USA) were mixed in a 3:5 ratio to create a homogeneous paste. The paste was stencil-printed and dried at 60 °C for 30 min. AglAgCl ink (Sigma-Aldrich, USA) was then painted onto the reference electrode and dried at 60 °C for 30 min. Double-sided adhesive wells (3 M, USA) were laser cut (8 mm in diameter) and adhered to the electrode surface, exposing the reference, counter, and working electrode (9 mm^2).

Electrochemical Immunoassay Protocol. The immunoassay and electrochemical detection mechanism are illustrated in Figure 1, and the protocol is as follows:

SPCE Functionalization. SPCEs were functionalized (see Figure S1) by covalently binding capture anti-N antibodies to the electrode surface via carbodiimide coupling using *N*-ethyl-*N*′-[3-(dimethylamino)propyl]carbodiimide/N-hydroxysuccinimide (EDC/NHS) chemistry. First, 20 μL of a solution of 5 mM EDC (Sigma-Aldrich, USA) and 5 mM NHS (Sigma-Aldrich, USA) in water was pipetted on the working electrode and incubated in a humid chamber for 45 min. Then, this solution was pipetted off, and 20 μL of the 10 μg/mL capture anti-N antibody in PBS was immediately added to the electrode surface. Following a 1 h incubation period in a humid chamber, the electrode was washed with PBST followed by PBS using solid stream spray bottles. The SPCE was then incubated with 50 μL of aged casein solution for 1 h to block non-specific activated binding sites and subsequently rinsed with PBST followed by PBS using transfer pipettes. The total duration for SPCE functionalization was 2 h and 45 min.

SPCE Testing. Functionalized SPCEs were tested by pipetting 20 μL of a sample solution onto the electrode surface. Following a 40 min incubation period, the electrodes were washed with PBST followed by PBS using solid stream spray bottles. Subsequently, 20 μL of a 0.5 μg/mL anti-N-HRP detection antibody solution prepared in HBSST was pipetted onto the electrode surface and incubated for 25 min. Following washing with PBST and PBS using solid stream spray bottles, 50 μL of TMB was added to the electrode surface and incubated for 2 min. Immediately following the TMB incubation, a chronoamperometry recording was started. Using a portable potentiostat (PalmSens4), a 0.0 V potential was applied to the working electrode (vs the AglAgCl reference electrode) for 2 min, while the current was recorded between the working and the counter electrodes. The total duration for SPCE testing was 70 min.

$$\Delta I = -(I_{100\ s}^{\text{sample}} - mean(I_{100\ s}^{\text{blank}}))$$

Data Analysis. Chronoamperometry traces were averaged on a 10 s interval (100 points) centered in 100 s following the start of the recording (I_{100s}). This 100 s timepoint was chosen to avoid the initial charging current and to evaluate the plateau current. Blank samples (n = 3), made with the same media as the samples tested but without the virus, were run in parallel to virus samples to get a measure of the background current. For every sample tested, the mean background current was subtracted from the sample current, and the immunoassay current output ΔI generated by each sample was defined as follows, as illustrated in Figure 1.

RESULTS AND DISCUSSION

Antibody Screening. Since the beginning of the pandemic, a large number of antibodies have become available for SARS-CoV-2, necessitating screening to optimize performance. To screen capture anti-N and detection anti-N-HRP antibodies, we performed the electrochemical immunoassay on our SPCEs using eight different antibody pairs (Table S1). The antibodies tested were selected based on a previous study[39] that identified commercially available antibodies that performed best on immunoassays targeting the SARS-CoV-2 N protein and following commercial supplier recommendations.[40] All antibody pairs from commercial sources (Pairs 2

https://doi.org/10.1021/acs.analchem.1c04966
Anal. Chem. 2022, 94, 4712−4719

to 8) were tested against in house-generated antibodies (Pair 1).

Figure 2 shows the immunoassay current output, ΔI, from a virus concentration of 5000 PFU/mL, generated using each of

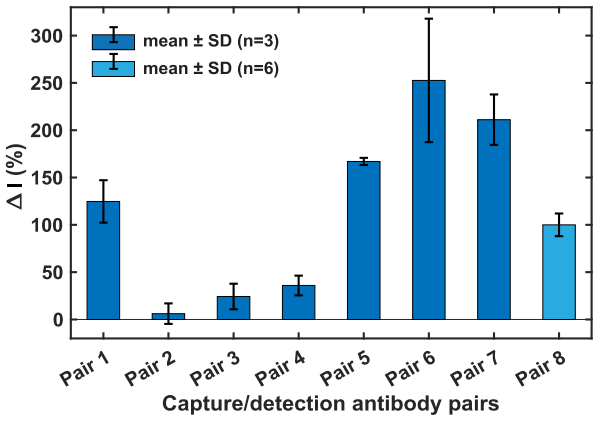

Figure 2. Comparison of capture/detection antibody pairs. Blank-subtracted current generated by SARS-CoV-2 samples at 5000 PFU/mL (2.4×10^8 RNA copies/mL), using different pairs of capture/detection antibodies. Antibody pairs are defined in Table S1. The data set was collected in two separate experiments, and measurements from Pair 8 were repeated across both experiments. For each pair, current is expressed as a percentage of the current generated using Pair 8 from the corresponding experiment. Except for Pair 8 where the current mean and standard deviation (SD) are calculated over both experiments (n = 6), data represent mean and SD of triplicate measurements (n = 3). SD of Pair 8 for each experiment (n = 3) remains higher than SD of Pair 5 (±11% and ±12% vs ±4%).

the eight antibody pairs. The results show that ΔI is highly variable across the eight antibody pairs tested, which is consistent with results from previous studies.[39,41] The difference in the signal observed across antibody pairs can be attributed to multiple factors, including the binding affinity between the antibodies and our target and the way the antibodies bind to the electrode surface. On our electrochemical immunoassay, Pair 5 gave a current output 34% higher than that generated by the affinity-purified rabbit anti-N polyclonal antibodies (Pair 1) and critically demonstrated the most consistent current output, as shown by the lowest standard deviation. Therefore, we identified Pair 5 as the antibody pair that performed best on our electrochemical immunoassay. From this point onward, all experiments were conducted with antibody Pair 5.

Electrochemical Response to Different Concentrations of SARS-CoV-2 Virus. The ability of our immunoassay to quantify the concentration of the SARS-CoV-2 virus in 20 μL of VTM-based samples was evaluated by exposing functionalized SPCEs to different inactivated SARS-CoV-2 virus concentrations. Chronoamperograms recorded from SPCEs exposed to eight different SARS-CoV-2 virus concentrations ranging from 0 to 110,000 PFU/mL are shown in Figure 3A. Each concentration was tested on three separate SPCEs (n = 3), and the average and standard deviation of the triplicate measurements are shown by line and shaded areas, respectively. The calibration curve generated by this data set is shown in Figure 3B. The graphs show clear separation between current responses to each concentration tested and an increase in ΔI with the increasing virus concentration. The current-to-concentration response curve

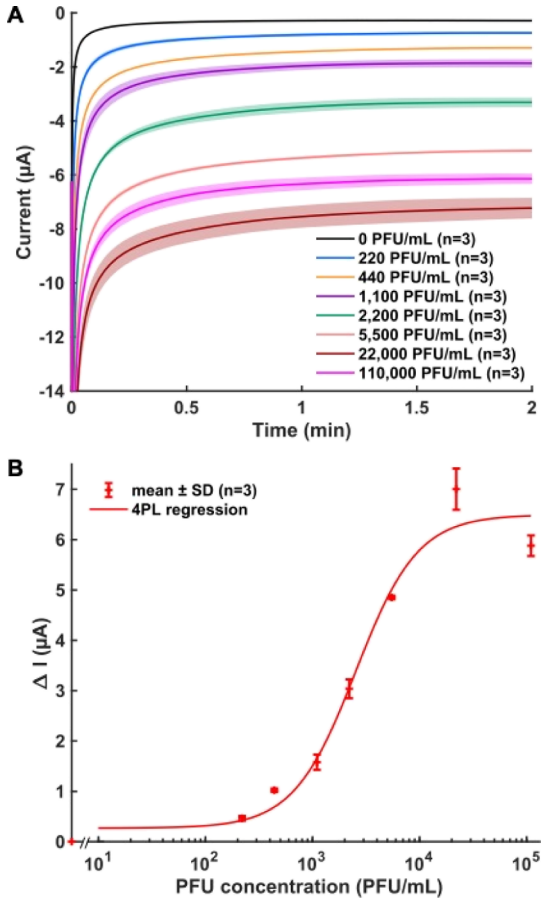

Figure 3. Electrochemical detection of the SARS-CoV-2 virus in 20 μL samples. (A) Chronoamperograms obtained from SPCEs exposed to different concentrations of the SARS-CoV-2 virus. Lines and shaded areas represent mean and SD of triplicate measurements, respectively. (B) Corresponding calibration curve showing ΔI averaged over a 10 s interval centered in t = 100 s. Data fitted with a 4-parameter logistic (4PL) regression. The LOD, calculated as the virus concentration corresponding to 3 SD of the blank signal, is equivalent to 45 PFU/mL [$\approx 2.17 \times 10^6$ viral RNA copies/mL, as calculated from the genome concentration of the virus stock solution which was measured via RT-digital droplet(dd)PCR].

follows a 4-parameter logistic (4PL) model, which is typical for immunoassays.[42,43] Note that the current response to the highest virus concentration tested, 110,000 PFU/mL, is lower than that of the lower 22,000 PFU/mL concentration. This could be attributed to the hook effect, which has been previously reported in immunoassays[44] when an overload of the virus prevents antibody binding and decreases complexation. Patient samples likely will not contain such high viral loads, but if a sample contained a viral load within the range impacted by the hook effect, the assay would still exhibit a positive result, and the accuracy of the test would not be compromised. These results demonstrate the ability of the immunoassay to quantify the SARS-CoV-2 virus concentration in VTM samples of volumes as low as 20 μL. The limit of detection (LOD) of our electrochemical assay, calculated as the viral concentration corresponding to three times the standard deviation of the signal recorded in the absence of the virus, was found to be equivalent to 45 PFU/mL. This calculated LOD is lower than the measured LOD of most commercially available rapid antigen tests, which are typically

https://doi.org/10.1021/acs.analchem.1c04966
Anal. Chem. 2022, 94, 4712−4719

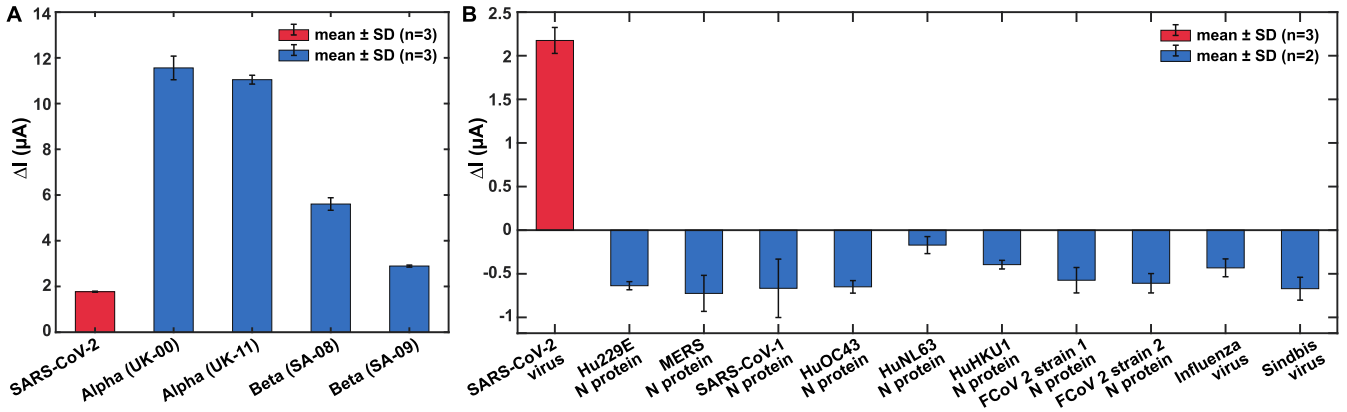

Figure 4. Cross-reactivity to SARS-CoV-2 variants and potential interferents in 20 μL VTM samples. (A) ΔI generated by virus samples of the SARS-CoV-2 original strain and SARS-CoV-2 variant strains. All samples were tested at 1100 PFU/mL as determined by a plaque assay, and corresponding viral RNA concentrations were 5.2×10^7, 2.0×10^9, 1.5×10^9, 1.8×10^7, and 1.7×10^7 copies/mL for SARS-CoV-2 original, alpha (UK-00), alpha (UK-11), beta (SA-08), and beta (SA-09) strains, respectively. Data represent mean and SD of triplicate measurements. (B) ΔI generated by virus samples of the SARS-CoV-2 original strain and samples of potential interfering viruses and recombinant N proteins from potential interfering viruses. SARS-CoV-2 original virus strain samples were tested at 1100 PFU/mL (5.2×10^7 RNA copies/mL), N-protein samples were tested at 100 ng/mL, and heterologous virus samples (influenza and Sindbis) were tested at 10,000 PFU/mL. Data represent mean and SD of triplicate measurements for the SARS-CoV-2 virus and duplicate measurements for potential interferents.

between 80 and 500 PFU/mL.[27,45] However, it is important to note that the lowest concentration tested as part of this experiment was 220 PFU/mL (Figure 3), which is above the calculated 45 PFU/mL LOD, whereas the LODs of the commercial tests reported in these studies[27,45] were measured concentrations. Nevertheless, the concentration of 220 PFU/mL that is clearly detected by our assay is well in the range of these reported LODs. Standard antigen capture ELISA was also performed on the same inactivated virus samples (Figure S2), with a LOD of 7 PFU/mL. Although it is lower than the LOD of the electrochemical assay, benefits of the electrochemical assay over ELISA include a reduced assay time from 24 h to less than 4 h (including surface functionalization), lower reagent volumes, and the use of portable recording instrumentation.

Cross-Reactivity to SARS-CoV-2 Variants and Potential Interferents. The ability to differentiate the target from other viruses while detecting SARS-CoV-2 variants is essential for test accuracy. Cross-reactivity studies using SARS-CoV-2 variant viruses and potential interferents were carried out to investigate the specificity of our biosensor toward SARS-CoV-2. Using the same experimental conditions as for SARS-CoV-2 detection (Figure 3), we tested the following four SARS-CoV-2 variants: Alpha (UK-00), Alpha (UK-11), Beta (SA-08), and Beta (SA-09) against the original SARS-CoV-2 strain on our functionalized SPCEs, as shown in Figure 4A. All virus strains were tested at the same concentration of 1,100 PFU/mL, and interestingly, all variant strains generated a higher signal than the original strain. This can be explained by the higher viral RNA content of the variant strains, as later revealed by RT-ddPCR assays (see Figure 4). Importantly, all four variants tested could be detected by our functionalized SPCEs indicating the applicability of the system as new variants emerge.

We then evaluated the response of our functionalized SPCEs to 10 potential interferents, including the influenza virus, Sindbis virus, and N proteins from 8 other coronaviruses as compared to the response generated by the SARS-CoV-2 virus. To simulate a worst-case scenario, potential interfering viruses and N proteins were tested at concentrations as high as 10,000 PFU/mL and 100 ng/mL, respectively, while the SARS-CoV-2 virus was tested at a clinically relevant concentration of 1100 PFU/mL.[46] Results from this interferent study are presented in Figure 4B and show that none of the 10 potential interferents tested were detected by our functionalized SPCEs. Instead, each of them generated a small negative ΔI, which means that their current response was closer to zero than that of the blank samples (VTMT only). This is likely due to proteins being present in such high concentrations in the potential interferent samples, which could block access of the detection antibodies to the electrode surface, decreasing the electron turnover by TMB. These results demonstrate the specificity of our assay toward the SARS-CoV-2 virus.

Proof-of-Concept Clinical Sample Study. To evaluate the diagnostic potential of our functionalized SPCEs on clinical samples, we carried out a proof-of-concept assay where we tested a total of 22 20-μL heat-inactivated de-identified nasopharyngeal samples that had been previously banked as part of a long-term care facility study (Table S2). All samples were tested with RT-qPCR and identified as either viral RNA negative or positive, according to their N1 cycle threshold (Ct) value ($\leq$38 or >38, respectively). Table 1 compares the results of this electrochemical assay to that of the RT-qPCR assay and shows specificity and sensitivity values, respectively, calculated as the number of samples identified as negatives by our electrochemical assay divided by the number of samples identified as negative by the RT-qPCR assay and the number of samples identified as positive by our electrochemical assay

Table 1. Clinical Nasopharyngeal Samples

electrochemical assay outcome	RT-qPCR assay outcome			
	positive			negative
	N1 Ct < 25	N1 Ct < 30	N1 Ct ≤ 38	N1 Ct > 38
positive	5	7	7	0
negative	0	3	6	9
		sensitivity		specificity
	100%	70%	54%	100%

https://doi.org/10.1021/acs.analchem.1c04966
Anal. Chem. 2022, 94, 4712−4719

divided by the number of samples identified as positive by the RT-qPCR assay. Our electrochemical assay was found to be 100% specific, with a total of 9 negative samples tested but only 54% sensitive when considering all 13 positive samples. However, the sensitivity of our assay increased with decreasing Ct values and reached 70 and 100% for samples with Ct values <30 and <25, respectively. This suggests that the LOD of our assay is around a Ct value of 25, which is defined as acceptable for a POC test by the WHO.[47] Because previous studies demonstrated that infectivity was significantly reduced when RT-qPCR Ct values were higher than 24,[48,49] these results suggest that our electrochemical assay has potential to be used as a method to identify SARS-CoV-2 infectious patients.

For samples in which the presence of the SARS-CoV-2 virus was detected by our electrochemical assay, the equivalent PFU concentration was quantified by simultaneously testing samples of the known PFU concentration on our assay, as shown in Figure S3. It is important to note that there could be discrepancies between the estimated equivalent PFU concentration and the N-protein concentration in these samples, justifying the use of the term "equivalent". Figure 5 shows the

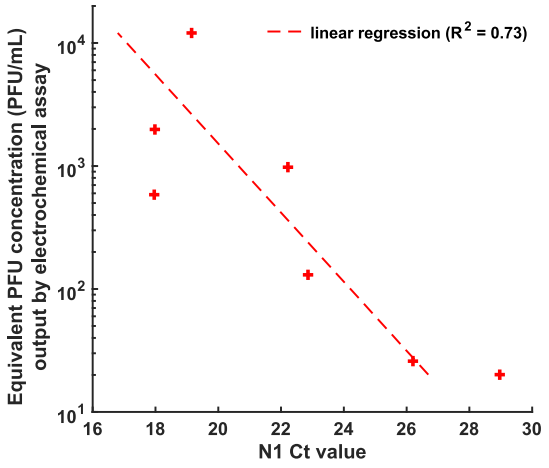

Figure 5. SARS-CoV-2 equivalent PFU concentrations of clinical nasopharyngeal samples from COVID-19 patients determined using our quantitative electrochemical assay, plotted against corresponding RT-qPCR N1 Ct values. The plot showing data from the 7 out of 10 samples tested with a N1 Ct value in the range 16−30 which were identified as positive by our electrochemical assay. Linear regression suggests a correlation between our assay output and the standard RT-qPCR Ct value (R^2 = 0.73). The difference can be attributed to the two assays measuring different aspects of the virus biochemistry (antigen content vs viral RNA).

equivalent PFU concentration of all seven samples that were identified as positive by our electrochemical assay, plotted against their N1 Ct value, as determined by the RT-qPCR assay.

The graph shows a possible linear correlation between both variables, with a coefficient of determination of 0.73. Because lower Ct values have been associated with higher chance of infectivity,[49,50] these results suggest that the output of our electrochemical assay could serve as a measure of patient infectivity. To test this hypothesis, plaque assays were performed on positive samples, and the actual PFU concentrations were compared to the PFU concentration equivalents output by our electrochemical assay. Note that the current response of our functionalized electrodes to a given virus concentration was more consistent in this assay than it was in the assay that generated the data shown in Figure 3 (as shown by the smaller error bars in Figure S3 compared to Figure 3), which resulted in a lower LOD (5.8 PFU/mL).

Figure 6 compares the results of our assay to those of plaque assays and shows a linear correlation between the equivalent

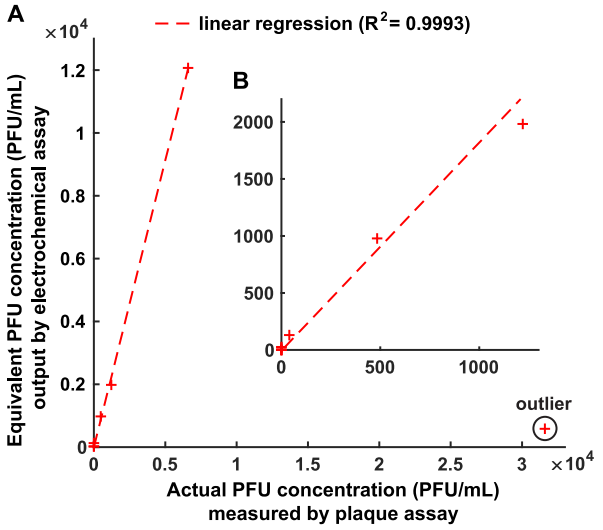

Figure 6. Correlation between the SARS-CoV-2 actual PFU concentration of RT-qPCR positive clinical nasopharyngeal samples obtained using a standard plaque assay and the equivalent PFU concentration of the same samples obtained using our electrochemical assay. The linear regression shown (R^2 = 0.9993) excludes the data point labeled as outlier. Out of the seven RT-qPCR positive samples that were identified as positive by our electrochemical assay, two of them were identified as non-infectious (0 PFU/mL) by the standard plaque assay. (A) Shows the entire data set, and (B) zooms in on lower PFU concentrations ranging from 0 to 1300 PFU/mL.

and the actual PFU concentrations obtained by the two methods, with a coefficient of determination of 0.9993. Note that one datapoint (circled, Figure 6) was excluded from the regression as it was identified as an outlier. The causes for this datapoint to be an outlier are unknown, and the sample could not be tested again due to limited available volume. It is possible that despite its high infectivity, this sample contained a lower amount of N proteins, which are the targeted molecules of the electrochemical assay. However, this sample was identified as infectious or positive by both methods. As shown in Table S2, the infectious samples with the two lowest actual PFU concentrations (measured by the plaque assay) had RT-qPCR N1 Ct values between 22 and 23, and no PFU was detected in samples with N1 Ct values higher than 23. However, according to our electrochemical assay, two positive samples with N1 Ct values of 26 and 29 were found to have equivalent PFU concentrations of 20 and 25 PFU/mL, respectively. This shows that our electrochemical immunoassay was able to detect the apparent SARS-CoV-2 virus in samples that the infectivity measure missed. Although a larger clinical study must be performed for this assay to be used as a diagnostic tool, these results indicate that our quantitative electrochemical assay may have potential to assess patient infectivity status.

https://doi.org/10.1021/acs.analchem.1c04966
Anal. Chem. 2022, 94, 4712−4719

CONCLUSIONS

Here, we have described a novel electrochemical biosensor for the detection of the SARS-CoV-2 N protein for practical applications in POC testing of COVID-19. We demonstrated successful functionalization of SPCEs using optimized antibody pairs, while reducing reagent use and time in comparison to traditional approaches such as ELISA and RT-qPCR. Furthermore, the assay can be fabricated at low cost (<$1, see Table S3) and would be easily scaled up for future manufacturing. The assay has been validated against inactivated SARS-CoV-2 virus samples, showing that the virus concentration can be quantified with a LOD that is lower than that of most rapid antigen tests currently on the market and that satisfies the WHO requirements for POC tests. A proof-of-concept clinical study was conducted on a small data set of 22 clinical samples, in which results from the assay developed herein were compared to those of both RT-qPCR and plaque assays. Despite these three assays measuring three different variables (antigen, genome copies, and infectivity), results from this proof-of-concept study show possible agreement between the developed assay and both RT-qPCR and plaque assays, indicating that the assay may have potential to predict infectivity of patients with COVID-19. A larger-scale clinical study would need to be conducted to confirm these preliminary findings. Current limitations of the assay include the manual pipetting steps needed to functionalize the electrodes and the time from the sample to result. Although assay time was greatly reduced compared to traditional lab-based methods such as ELISA, RT-qPCR, and plaque assays, time from the sample to the result remains approximately 70 min. Future work is aimed at automating the assay by integrating it in a fluidic platform amenable to the point of care,[51] further reducing the assay time, and assessing the stability of the functionalized SPCEs over extended time periods under various storage conditions. This will enable the assay to be integrated into a robust, quantitative, and sensitive POC test for the detection of SARS-CoV-2 infection in patients.

ASSOCIATED CONTENT

Supporting Information

The Supporting Information is available free of charge at https://pubs.acs.org/doi/10.1021/acs.analchem.1c04966.

Schematics of the SPCE functionalization process, ELISA validation of inactivated SARS-CoV-2 samples, clinical sample analysis, description of antibody pairs tested, and clinical study results (PDF)

AUTHOR INFORMATION

Corresponding Author

Charles S. Henry − *Department of Chemistry, Colorado State University, Fort Collins, Colorado 80523, United States; Department of Chemical and Biological Engineering and School of Biomedical Engineering, Colorado State University, Fort Collins, Colorado 80523, United States;* orcid.org/0000-0002-8671-7728; Email: chuck.henry@colostate.edu

Authors

Isabelle C. Samper − *Department of Chemistry, Colorado State University, Fort Collins, Colorado 80523, United States; Department of Chemical and Biological Engineering, Colorado State University, Fort Collins, Colorado 80523, United States*

Catherine J. McMahon − *Department of Chemistry, Colorado State University, Fort Collins, Colorado 80523, United States*

Melissa S. Schenkel − *Department of Chemistry, Colorado State University, Fort Collins, Colorado 80523, United States*

Kaylee M. Clark − *Department of Chemistry, Colorado State University, Fort Collins, Colorado 80523, United States*

Wisarut Khamcharoen − *Department of Chemistry, Faculty of Science, Srinakharinwirot University, Bangkok 10110, Thailand*

Loran B. R. Anderson − *Department of Microbiology, Immunology, and Pathology, Colorado State University, Fort Collins, Colorado 80523, United States*

James S. Terry − *Department of Microbiology, Immunology, and Pathology, Colorado State University, Fort Collins, Colorado 80523, United States*

Emily N. Gallichotte − *Department of Microbiology, Immunology, and Pathology, Colorado State University, Fort Collins, Colorado 80523, United States*

Gregory D. Ebel − *Department of Microbiology, Immunology, and Pathology, Colorado State University, Fort Collins, Colorado 80523, United States*

Brian J. Geiss − *Department of Microbiology, Immunology, and Pathology and School of Biomedical Engineering, Colorado State University, Fort Collins, Colorado 80523, United States*

David S. Dandy − *Department of Chemical and Biological Engineering and School of Biomedical Engineering, Colorado State University, Fort Collins, Colorado 80523, United States*

Complete contact information is available at: https://pubs.acs.org/10.1021/acs.analchem.1c04966

Author Contributions

I.C.S. and C.J.M. contributed equally. The article was written through contributions of all authors. All authors have given approval to the final version of the article.

Notes

The authors declare no competing financial interest.

ACKNOWLEDGMENTS

This work has been supported by Colorado State University, the State of Colorado Office of Economic Development, the International Trade Advanced Industries Accelerator, the NIH (R01 EB031510-01 and R01 AI132668), the Science Achievement Scholarship of Thailand, and Balanced Biotech Inc.

REFERENCES

(1) de Eguilaz, M. R.; Cumba, L. R.; Forster, R. J. *Electrochem. Commun.* **2020**, *116*, 106762.

(2) Kaushik, A.; Yndart, A.; Kumar, S.; Jayant, R. D.; Vashist, A.; Brown, A. N.; Li, C.-Z.; Nair, M. *Sci. Rep.* **2018**, *8*, 9700.

(3) Li, X.; Scida, K.; Crooks, R. M. *Anal. Chem.* **2015**, *87*, 9009−9015.

(4) Zhou, L.; Huang, J.; Yu, B.; Liu, Y.; You, T. *ACS Appl. Mater. Interfaces* **2015**, *7*, 24438−24445.

(5) Shrivastav, A. M.; Cvelbar, U.; Abdulhalim, I. *Commun. Biol.* **2021**, *4*, 70.

(6) St John, A.; Price, C. P. *Clin. Biochem. Rev.* **2014**, *35*, 155−167.

(7) Mejía-Salazar, J. R.; Rodrigues Cruz, K.; Materón Vásques, E. M.; Novais de Oliveira, O., Jr. *Sensors* **2020**, *20*, 1951.

(8) Menon, S.; Mathew, M. R.; Sam, S.; Keerthi, K.; Kumar, K. G. *J. Electroanal. Chem.* **2020**, *878*, 114596.

(9) Electrochemical Glucose Biosensors | Chemical Reviews. https://pubs-acs-org.ezproxy2.library.colostate.edu/doi/full/10.1021/cr068123a (accessed Oct 6, 2021).
(10) Godino, N.; Gorkin, R.; Bourke, K.; Ducrée, J. *Lab Chip* **2012**, *12*, 3281−3284.
(11) Metters, J. P.; Banks, C. E.; Banks, C. E. *Analyst* **2014**, *139*, 3999−4004.
(12) Yáñez-Sedeño, P.; Campuzano, S.; Pingarrón, J. M. *Biosensors* **2020**, *10*, 76.
(13) WHO Coronavirus (COVID-19) Dashboard. https://covid19.who.int (accessed Sept 9, 2021).
(14) Loeffelholz, M. J.; Tang, Y.-W. *Emerging Microbes Infect.* **2020**, *9*, 747−756.
(15) Vandenberg, O.; Martiny, D.; Rochas, O.; van Belkum, A.; Kozlakidis, Z. *Nat. Rev. Microbiol.* **2021**, *19*, 171−183.
(16) Valera, E.; Jankelow, A.; Lim, J.; Kindratenko, V.; Ganguli, A.; White, K.; Kumar, J.; Bashir, R. *ACS Nano* **2021**, *15*, 7899−7906.
(17) Choi, J. R. *Front. Chem.* **2020**, *8*, 517.
(18) Souf, S. *Biosci. Horiz.* **2016**, *9*, hzw010.
(19) Voller, A.; Bartlett, A.; Bidwell, D. E.; Clark, M. F.; Adams, A. N. *J. Gen. Virol.* **1976**, *33*, 165−167.
(20) Yolken, R. H. *Yale J. Biol. Med.* **1980**, *53*, 85−92.
(21) Boonham, N.; Kreuze, J.; Winter, S.; van der Vlugt, R.; Bergervoet, J.; Tomlinson, J.; Mumford, R. *Virus Res.* **2014**, *186*, 20−31.
(22) Scourfield, D. O.; Reed, S. G.; Quastel, M.; Alderson, J.; Bart, V. M. T.; Teijeira Crespo, A.; Jones, R.; Pring, E.; Richter, F. C.; The Oxford-Cardiff COVID-19 Literature Consortium; Burnell, S. E. A. The Role and Uses of Antibodies in COVID-19 Infections: A Living Review. *Oxf. open immunol.* **2021**, *2* (). https://doi.org/DOI: 10.1093/oxfimm/iqab003.
(23) Peeling, R. W.; Wedderburn, C. J.; Garcia, P. J.; Boeras, D.; Fongwen, N.; Nkengasong, J.; Sall, A.; Tanuri, A.; Heymann, D. L. *Lancet Infect. Dis.* **2020**, *20*, e245−e249.
(24) CDC. Healthcare Workers. https://www.cdc.gov/coronavirus/2019-ncov/hcp/testing-overview.html (accessed Sept 9, 2021).
(25) BinaxNOW. http://binaxnow.workplace.abbott/binaxnow-3 (accessed Oct 7, 2021).
(26) InteliSwab—COVID Rapid Test. Results in hand, in minutes. https://inteliswab.com/ (accessed Oct 7, 2021).
(27) Cubas-Atienzar, A. I.; Kontogianni, K.; Edwards, T.; Wooding, D.; Buist, K.; Thompson, C. R.; Williams, C. T.; Patterson, E. I.; Hughes, G. L.; Baldwin, L.; Escadafal, C.; Sacks, J. A.; Adams, E. R. *Sci. Rep.* **2021**, *11*, 18313.
(28) Campuzano, S.; Pedrero, M.; Yáñez-Sedeño, P.; Pingarrón, J. M. *Sens. Actuators, B* **2021**, *345*, 130349.
(29) Pashchenko, O.; Shelby, T.; Banerjee, T.; Santra, S. *ACS Infect. Dis.* **2018**, *4*, 1162−1178.
(30) Li, T.; Wang, L.; Wang, H.; Li, X.; Zhang, S.; Xu, Y.; Wei, W. *Front. Cell. Infect. Microbiol.* **2020**, *10*, 470.
(31) Shan, D.; Johnson, J. M.; Fernandes, S. C.; Suib, H.; Hwang, S.; Wuelfing, D.; Mendes, M.; Holdridge, M.; Burke, E. M.; Beauregard, K.; Zhang, Y.; Cleary, M.; Xu, S.; Yao, X.; Patel, P. P.; Plavina, T.; Wilson, D. H.; Chang, L.; Kaiser, K. M.; Nattermann, J.; Schmidt, S. V.; Latz, E.; Hrusovsky, K.; Mattoon, D.; Ball, A. J. *Nat. Commun.* **2021**, *12*, 1931.
(32) CDC Posts New Standard Operating Procedure for Creating Viral Transport Media https://www.cdc.gov/csels/dls/locs/2020/new_sop_for_creating_vtm.html (accessed Nov 2, 2021).
(33) Fagre, A.; Lewis, J.; Eckley, M.; Zhan, S.; Rocha, S. M.; Sexton, N. R.; Burke, B.; Geiss, B.; Peersen, O.; Bass, T.; Kading, R.; Rovnak, J.; Ebel, G. D.; Tjalkens, R. B.; Aboellail, T.; Schountz, T. *PLoS Pathog.* **2021**, *17*, No. e1009585.
(34) Terry, J. S.; Anderson, L. B.; Scherman, M. S.; McAlister, C. E.; Perera, R.; Schountz, T.; Geiss, B. J. *Virology* **2021**, *558*, 28−37.
(35) Grant, B. D.; Anderson, C. E.; Williford, J. R.; Alonzo, L. F.; Glukhova, V. A.; Boyle, D. S.; Weigl, B. H.; Nichols, K. P. *Anal. Chem.* **2020**, *92*, 11305−11309.
(36) Case, J. B.; Bailey, A. L.; Kim, A. S.; Chen, R. E.; Diamond, M. S. *Virology* **2020**, *548*, 39−48.
(37) Gallichotte, E. N.; Quicke, K. M.; Sexton, N. R.; Fitzmeyer, E.; Young, M. C.; Janich, A. J.; Dobos, K.; Pabilonia, K. L.; Gahm, G.; Carlton, E. J.; Ebel, G. D.; Ehrhart, N. *Microbiol. Spectrum* **2021**, *9*, No. e01003.
(38) Kava, A. A.; Beardsley, C.; Hofstetter, J.; Henry, C. S. *Anal. Chim. Acta* **2020**, *1103*, 58−66.
(39) Cate, D. M.; Bishop, J. D.; Hsieh, H. V.; Glukhova, V. A.; Alonzo, L. F.; Hermansky, H. G.; Barrios-Lopez, B.; Grant, B. D.; Anderson, C. E.; Spencer, E.; Kuhn, S.; Gallagher, R.; Rivera, R.; Bennett, C.; Byrnes, S. A.; Connelly, J. T.; Dewan, P. K.; Boyle, D. S.; Weigl, B. H.; Nichols, K. P. *ACS Omega* **2021**, *6*, 25116−25123.
(40) A Complete Toolkit to Develop a Diagnostic SARS-CoV-2 Antigen Test. https://www.sinobiological.com/research/virus/immunodiagnostic-sars-cov-2-antigen-test (accessed Oct 11, 2021).
(41) *Lateral Flow Immunoassay*; Wong, R., Tse, H., Eds.; Humana Press: Totowa, NJ, 2009.
(42) O'Connell, M. A.; Belanger, B. A.; Haaland, P. D. *Chemom. Intell. Lab. Syst.* **1993**, *20*, 97−114.
(43) Heineman, W. R.; Halsall, H. B. *Anal. Chem.* **1985**, *57*, 1321A−1331A.
(44) Tate, J.; Ward, G. *Clin. Biochem. Rev.* **2004**, *25*, 105−20.
(45) Corman, V. M.; Haage, V. C.; Bleicker, T.; Schmidt, M. L.; Mühlemann, B.; Zuchowski, M.; Jo, W. K.; Tscheak, P.; Möncke-Buchner, E.; Müller, M. A.; Krumbholz, A.; Drexler, J. F.; Drosten, C. *Lancet Microbe* **2021**, *2*, e311−e319.
(46) Lin, Y.-C.; Malott, R. J.; Ward, L.; Kiplagat, L.; Pabbaraju, K.; Gill, K.; Berenger, B. M.; Hu, J.; Fonseca, K.; Noyce, R.; Louie, T.; Evans, D. H.; Conly, J. M. *Detection and Quantification of Infectious Severe Acute Respiratory Coronavirus-2 in Diverse Clinical and Environmental Samples from Infected Patients: Evidence to Support Respiratory Droplet, and Direct and Indirect Contact as Significant Modes of Transmission*, 2021; p 2021.
(47) World Health Organization. *Target Product Profiles for Priority Diagnostics to Support Response to the COVID-19 Pandemic v.1.0*; World Health Organization, September 28, 2020.
(48) Rao, S. N.; Manissero, D.; Steele, V. R.; Pareja, J. *Infect. Dis. Ther.* **2020**, *9*, 573−586.
(49) Bullard, J.; Dust, K.; Funk, D.; Strong, J. E.; Alexander, D.; Garnett, L.; Boodman, C.; Bello, A.; Hedley, A.; Schiffman, Z.; Doan, K.; Bastien, N.; Li, Y.; Van Caeseele, P. G.; Poliquin, G. *Clin. Infect. Dis.* **2020**, *71* (10), 2663−2666.
(50) Laferl, H.; Kelani, H.; Seitz, T.; Holzer, B.; Zimpernik, I.; Steinrigl, A.; Schmoll, F.; Wenisch, C.; Allerberger, F. *Infection* **2021**, *49*, 95−101.
(51) Samper, I. C.; Sánchez-Cano, A.; Khamcharoen, W.; Jang, I.; Siangproh, W.; Baldrich, E.; Geiss, B. J.; Dandy, D. S.; Henry, C. S. *ACS Sens.* **2021**, *6*, 4067.

https://doi.org/10.1021/acs.analchem.1c04966
Anal. Chem. 2022, 94, 4712−4719